Temperature determined by isobaric yield ratios in heavy-ion collisions

C. W. Ma (马春旺),[1,*] J. Pu (普洁),[1,2] Y. G. Ma (马余刚),[2,†] R. Wada,[3,‡] and S. S. Wang (王闪闪)[1]
[1]*Department of Physics, Henan Normal University, Xinxiang 453007, China*
[2]*Shanghai Institute of Applied Physics, Chinese Academy of Sciences, Shanghai 201800, China*
[3]*Institute of Modern Physics HIRFL, Chinese Academy of Sciences, Lanzhou 730000, China*
(Received 6 September 2012; revised manuscript received 20 October 2012; published 30 November 2012)

Background: Temperature (T) in heavy-ion collisions is an important parameter. Previously, many works have focused on the temperature of the hot emitting source. But there are few systematic studies of the temperature among heavy fragments in peripheral collisions with incident energies near the Fermi energy to a few A GeV, though it is very important to study the property of neutron-rich nucleus in heavy-ion collisions.
Purpose: This work focuses on the study of temperature associated with the final heavy fragments in reactions induced by both the neutron-proton symmetric and the neutron-rich projectiles, and with incident energy ranges from 60A MeV to 1A GeV.
Methods: Isobaric yield ratio (IYR) is used to determine the temperature of heavy fragments. Cross sections of measured fragments in reactions are analyzed, and a modified statistical abrasion-ablation (SAA) model is used to calculate the yield of fragment in 140A MeV ^{64}Ni + ^{9}Be and 1A GeV ^{136}Xe + ^{208}Pb reactions.
Results: Relatively low T of heavy fragments are obtained in different reactions (T ranges from 1 to 3 MeV). T is also found to depend on the neutron richness of the projectile. The incident energy affects T very little. $\Delta\mu/T$ (the ratio of the difference between the chemical potential of neutron and proton to temperature) is found to increase linearly as N/Z of projectile increases. It is found that T of the ^{48}Ca reaction, for which IYRs are $A < 50$ isobars, is affected greatly by the temperature-corrected $\Delta B(T)$. But T of reactions using IYRs of heavier fragments are only slightly affected by the temperature-corrected $\Delta B(T)$. The SAA model analysis gives a consistent overview of the results extracted in this work.
Conclusions: T from IYR, which is for secondary fragments, is different from that of the hot emitting source. T and $\Delta\mu$ are essentially governed by the sequential decay process.

DOI: 10.1103/PhysRevC.86.054611 PACS number(s): 25.70.Pq, 21.65.Cd, 25.70.Mn

I. INTRODUCTION

In heavy-ion collisions (HICs) above the intermediate energy (with incident energy $> 20A$ MeV), the temperature T is high enough to provide the environment for nuclear liquid-gas transition. Many works have focused on the critical point in T experimentally [1–8] and theoretically [9,10]. T is also important in determining the symmetry energy of a neutron-rich nucleus [11–15]. Due to the complexity of the HIC processes and the importance of T, many methods have been developed to obtain T from thermal energy [16], excitation energy [17–20], isotopic yields (Albergo thermometer) [8,21–26], and kinetic energy spectra [27–29]. T based on these methods have differences but can be related to each other [19,29].

The yield of a fragment in a HIC, on the one hand, is greatly influenced by T, and on the other hand, is determined by its free energy due to nonzero T [1]. Thus the yield of a fragment can constrain both its binding energy and T. In some models which estimate isotopic yield, T is an important parameter [30–33], while in other works the isotopic yield is also used to estimate the binding energy of unknown isotopes [30]. In works using the yield of a fragment to constrain the binding energy, for example, in the study of the symmetry energy of fragments, it is proposed that the isobaric yield ratio cancels out the energy term which only depends on the mass of fragment, thus the specific energy term can be extracted [34,35]. But the shortcoming of this method is that the coefficient of energy term and T cannot be separated, thus they must be viewed as whole parameters, for example, in the study of the symmetry-energy coefficients to T ($a_{\rm sym}/T$) of the neutron-rich nucleus [34,36–38]. If the binding energy of fragment at nonzero T is known, the yield of a fragment can also be used to determine T. One point to remember is that the measured heavy fragment in a HIC undergoes the sequential decay and deexcitation processes, which makes it cool down. T of a heavy fragment should be quite lower than that of the hot emitting source [17,39].

Based on the free energy, the modified Fisher model (MFM) well describes the isotopic yield distributions of intermediate mass fragments produced in proton-induced multifragmentation at relativistic energies [1,40]. The MFM has been used to study the behavior of fragments near the critical point of the liquid-gas transition [3,5–8]. In the MFM, the yield of an isotope is determined by chemical potential, free energy, and entropy. In this article, we will use the isobaric yield ratio to extract T in HICs. The article is organized as follows: First, we briefly introduce the isobaric ratio method based on the MFM. Second, we verify that the binding energy of nucleus at zero temperature can be used instead in the isobaric ratio method.

*machunwang@126.com
†ygma@sinap.ac.cn
‡wada@comp.tamu.edu

At last, T determined by isobaric yield will be shown and the results will be discussed.

II. ISOBARIC YIELD RATIO METHOD

Following the MFM [1,40], the generalized expression of the yield of a fragment with mass A and neutron-excess $I (I \equiv N - Z)$ is

$$Y(A, I) = CA^{-\tau} \exp\{[W(A, I) + \mu_n N + \mu_p Z]/T + N \ln(N/A) + Z \ln(Z/A)\}, \quad (1)$$

where C is a constant. The $A^{-\tau}$ term originates from the entropy of the fragment, τ's for all fragments are identical. μ_n and μ_p are the neutron and proton chemical potentials, respectively, and $W(A, I)$ is the Helmholtz free energy of the cluster (fragment). In principle Eq. (1) should be applied to hot nuclear matter near the critical point. However, when Eq. (1) was applied to the cold fragments in Ref. [41], they showed that useful information can be extracted to elucidate the effects of the secondary decay process. In that case, T and other parameters do not correspond to those in the primary hot nuclear matter but do correspond to those modified by the secondary decay process. Therefore it is still useful to apply Eq. (1) to the experimentally observed cold fragments to elucidate the effect of the sequential process on the characteristic physical parameters, such as T or chemical potential, as discussed below.

Defining the yield ratio between isobars differing by 2 units in I, we have

$$R(I + 2, I, A) = Y(A, I + 2)/Y(A, I) = \exp\{[W(I + 2, A) - W(I, A) + \Delta\mu]/T + S_{\rm mix}(I + 2, A) - S_{\rm mix}(I, A)\}, \quad (2)$$

where $S_{\rm mix}(I, A) = N\ln(N/A) + Z\ln(Z/A)$, and $\Delta\mu = \mu_n - \mu_p$. Taking the logarithm of $R(I + 2, I, A)$, one obtains

$$\ln R(I + 2, I, A) - \Delta S = (\Delta W + \Delta\mu)/T, \quad (3)$$

where $\Delta S = S_{\rm mix}(I + 2, A) - S_{\rm mix}(I, A)$, and $\Delta W = W(I + 2, A) - W(I, A)$ is the difference between the free energies of isobars. $W(I, A)$ is supposed to equal the binding energy B of a fragment at given T and density ρ [1] [written as $B(\rho, T)$]. If $B(\rho, T)$ (which includes the contributions from the binding energy and entropy) is known, T and $\Delta\mu$ can be obtained using the isobaric yield ratio (IYR) from Eq. (3).

The known B of the nucleus is for $T = 0$ [written as $B(0)$]. When $T \neq 0$, entropy contributes to the binding energy [written as $B(T)$] and makes $B(0) \neq B(T)$. The other good news is that since ΔW can serve as the independent variable, actually $B(T)$ is not important anymore in Eq. (3). If $B(0)$ can be used instead of $B(T)$ in the calculation of ΔW, the temperature of the fragment can be extracted using Eq. (3). Thus before determining T using the IYR method, whether $\Delta B(0) = \Delta B(T)$ should be evaluated [$\Delta B(T) = B_{(I+2)}(T) - B_{(I)}(T)$ is the difference between the binding energies of the $I + 2$ and I isobars].

Using the density-functional theory based on the Skyrme interaction (SKM), the T dependence of the binding energy of a finite nucleus has been proposed to be [42]

$$B(A, I, T) = -(15.31 - 0.04T^2)A + (18.30 + 0.50T^2)A^{2/3} + (19.69 + 0.42T^2)I^2/A - (33.18 + 2.06T^2)I^2/A^{4/3} + E_c\frac{Z^2}{A^{1/3}} + E_{\rm dif}\frac{Z^2}{A} + E_{\rm ex}\frac{Z^{4/3}}{A^{1/3}} + \Delta(N, Z), \quad (4)$$

where $E_{\rm dif}$ and $E_{\rm ex}$ are the coefficients for the diffuseness correction and the exchange correlation to the Coulomb energy. $\Delta(N, Z)$ is the pairing-energy term.

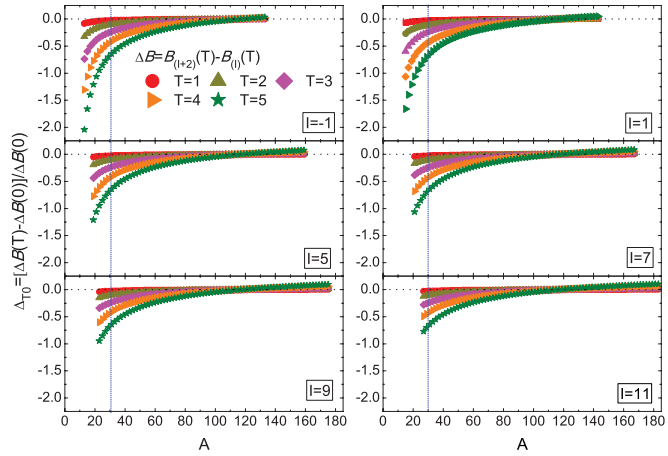

FIG. 1. (Color online) $\Delta_{T0} \equiv [\Delta B(T) - \Delta B(0)]/\Delta B(0)$ of isobars with I from -1 to 11 at different T. $\Delta B(T)$ is the difference between the binding energies of the $I + 2$ and I isobars at T. $\Delta B(T) = B_{(I+2)}(T) - B_{(I)}(T)$.

The binding energy of the nucleus at T from 0 to 5 MeV are calculated using Eq. (4). To see how fast $\Delta B(T)$ between isobars increases with temperature, the values of $\Delta_{T0} \equiv [\Delta B(T) - \Delta B(0)]/\Delta B(0)$ are plotted in Fig. 1. At $T \sim 1$ MeV, Δ_{T0} of the $I = -1 \sim 11$ isobars are very close to zero. Δ_{T0} decreases as the mass becomes larger, i.e., the larger the A of the nucleus, the closer Δ_{T0} is to 0. For isobars of small mass, Δ_{T0} decreases similarly as T decreases. At $T \geqslant 3$ MeV, the $A < 50$ isobars show relatively large Δ_{T0} ($\Delta_{T0} < -0.1$ corresponds to uncertainty larger than 10%). $\Delta B(T)$ of $A < 50$ isobars should be used more carefully around $T \geqslant 3$ MeV. In Eq. (3) ΔW is the difference between free energies of isobars, thus the very little Δ_{T0} for $I \geqslant 5$ and $A > 50$ isobars occurs when $\Delta B(T)$ is replaced by $\Delta B(0)$, and we need not know the actual $B(T)$. The smaller Δ_{T0} of isobars at T, the closer T obtained from Eq. (3) approximates the real value. Thus theoretically, the yield ratios of $I \geqslant 5$ isobars are suitable observables to extract T. Replacing the ΔW term in Eq. (3) by $\Delta B(0)$ (hereafter denoted as ΔB), one obtains

$$\ln R(I + 2, I, A) - \Delta S = (\Delta B + \Delta\mu)/T. \quad (5)$$

III. RESULTS AND DISCUSSIONS

By analyzing IYRs in HICs, T and $\Delta\mu$ can be determined using Eq. (5). The analysis is performed using the IYRs of $I \geqslant 5$ isobars. First, the dependence of T on I is investigated

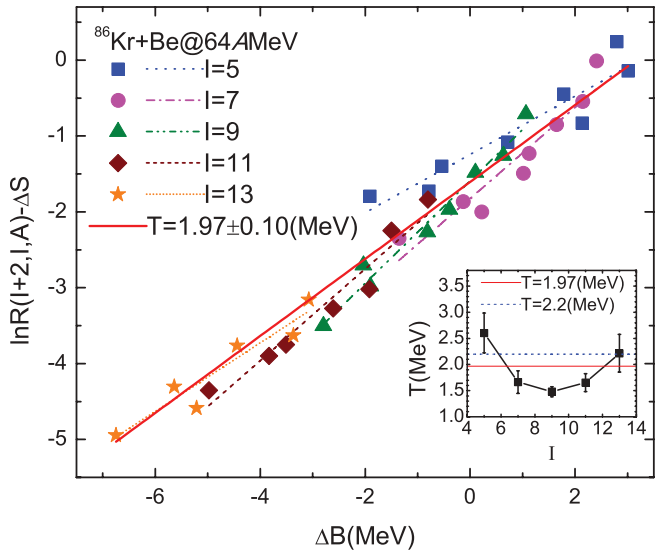

FIG. 2. (Color online) The correlation between IYR and ΔB of isobars in the 64A MeV ^{86}Kr + ^{9}Be projectile fragmentation reaction [43]. The lines are the fitting results of IYRs using Eq. (5). The solid line represents the fitting line of all the data. The inserted figure shows the fitted values of T, in which the solid line represents T fitted from all the data, and the dotted line represents $T = 2.2$ MeV used in Ref. [30].

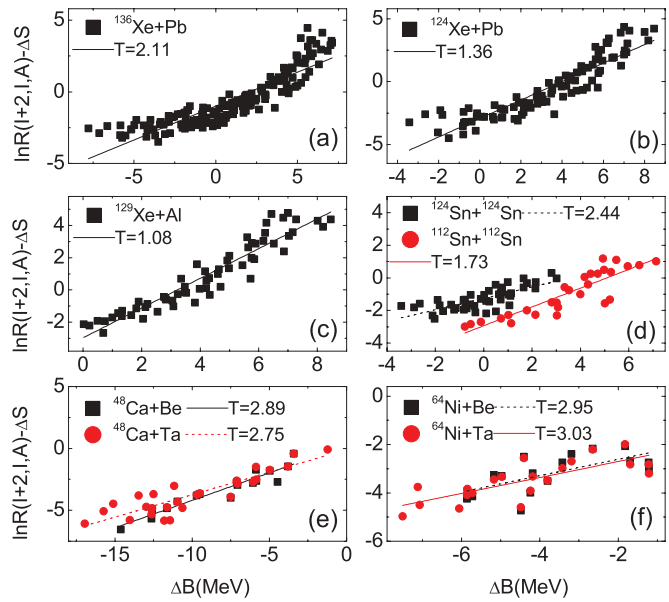

FIG. 3. (Color online) The correlation between IYR and ΔB of isobars in the following reactions: (a) 1A GeV ^{136}Xe + Pb [45], (b) 1A GeV ^{124}Xe + Pb [45], (c) 790A MeV ^{129}Xe + Al [46], (d) 1A GeV ^{112}Sn + ^{112}Sn and ^{124}Sn + ^{124}Sn [47], (e) 140A MeV ^{48}Ca + ^{9}Be/^{181}Ta [48], and (f) 140A MeV ^{64}Ni + ^{9}Be/^{181}Ta [48]. ΔB is calculated using the experimental binding energy of the nucleus in Ref. [44]. The lines denote the fitting results using Eq. (5) and T is the temperature obtained.

using the data in the 64A MeV ^{86}Kr + ^{9}Be projectile fragmentation reaction [43]. IYRs of isobars are plotted in Fig. 2, which almost overlap except the IYR of $I = 5$. ΔB are calculated using the experimental binding energy of the nucleus in Ref. [44]. The IYRs are fitted individually using Eq. (5) according to each I, and all the data are also fitted as a whole (shown as the solid line). The fitted values of T are plotted in the inserted figure. Relatively similar T are obtained from $I \geqslant 5$ IYR. The line in the inserted figure represents T fitted from all the IYR data.

To see T extracted from IYRs more systematically, IYRs in reactions of the 1A GeV ^{124,136}Xe [45], 790A MeV ^{129}Xe [46], 1A GeV ^{112,124}Sn [47], and 140A MeV ^{48}Ca and ^{64}Ni [48], are investigated. The results are plotted in Fig. 3. All the IYRs of isobars with different I are fitted as a whole and T obtained are given in each panel. IYRs in these reactions can be well fitted using Eq. (5). T and $\Delta\mu$ obtained are plotted in Fig. 4. The line in Fig. 4(a) is the average value of T in these reactions, which is $T = 2.23$ MeV. By analyzing the results of T, the conclusions below can be drawn:

(i) Relatively low T, which range from 1 to 3 MeV, are found in these reactions.

(ii) The neutron richness of projectile affects T. T of a neutron-rich reaction system is higher than that of the neutron-proton symmetric reaction systems when similar measurements are made, i.e., $T(^{136}\text{Xe}) > T(^{124}\text{Xe})$, and $T(^{124}\text{Sn}) > T(^{112}\text{Sn})$. This is a similar phenomenon as the isospin dependence of the fragment yields measured in reactions of neutron-proton symmetric and neutron-rich reactions [49]. The isotopic temperature (T_{HeLi}) was also found to increase when the projectile becomes more neutron rich using the isospin-dependent quantum molecular dynamics model [50].

(iii) The mass of target affects T very slightly. T obtained from the ^{48}Ca + ^{9}Be/^{181}Ta reaction are very similar. A similar observation in T is made in the ^{64}Ni + ^{9}Be/^{181}Ta reaction.

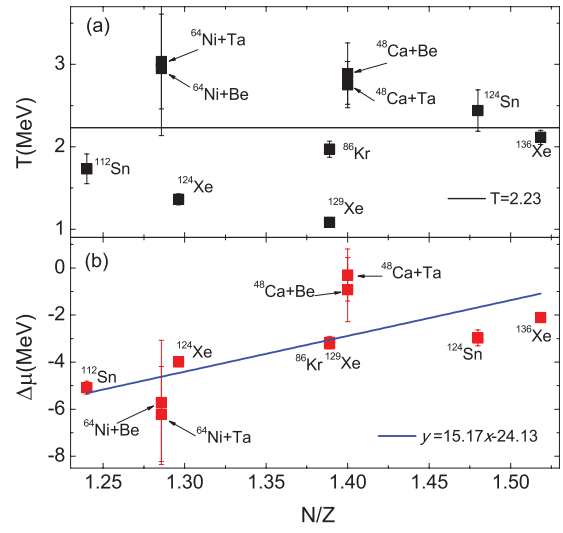

FIG. 4. (Color online) (a) The fitted temperature T, and (b) $\Delta\mu$ from IYRs in reactions analyzed in Fig. 3. $\Delta\mu$ of the ^{86}Kr and ^{129}Xe reactions overlaps. The solid line in (a) represents the average value of T, and the line in (b) is the result of the linear fit between $\Delta\mu$ and N/Z.

(iv) The incident energy of the reaction, which ranges from 64A MeV to 1A GeV, does not influence T very much. This occurs, as shown later using a modified statistical abrasion-ablation model analysis, because T is essentially governed by the sequential decay process.

T determined from IYRs of heavy fragments is lower than that from the Albergo isotopic temperatures of light fragments ($T_{\rm HHe}$) and slope temperatures ($T_{\rm slope}$) from the energy spectrum [19,24], but is close to the isotopic temperatures involving heavier isotopes ($T_{\rm BeHe}$, $T_{\rm LiBe}$, $T_{\rm BeLi}$, $T_{\rm LiLi}$ [25], and $T_{\rm CC}$ [51]). In a sequential decay process, light particles, such as p, n, and α, are emitted. When the light particle emission ceases, the fragment can still emit γ rays and it further cools off. The extracted low temperatures associated with heavy fragments for the reactions in the wide incident energy range indicate the dominance of the secondary decay effect on the temperature. One can also see the systematic trend that the temperatures from the lighter system tend to be higher than those of the heavier systems. Even though the MFM method provides a crude way to evaluate the temperatures, they are still useful in elucidating the entire process of the fragment production.

μ_n, μ_p, and $\Delta\mu$ are associated with the properties of the emitting source but not the fragments themselves [1,40]. Relatively large $\Delta\mu$ were observed in this analysis for the reactions. A linear correlation is found between the correlation of $\Delta\mu$ and N/Z of the projectile, which is shown as the solid line in Fig. 4(b). The linear fitting result between $\Delta\mu$ and N/Z reads $y = (15.21 \pm 5.82)x + (-24.16 \pm 7.97)$.

Rewriting Eq. (5), we get the following form

$$\ln R(I+2, I, A) - \Delta S - \Delta\mu/T = \Delta B/T, \qquad (6)$$

with the left-hand side involving IYR and $\Delta\mu$, which relate to each reaction; the right-hand side associates with $\Delta B/T$ of the isobars. For simplification, the left-hand side of Eq. (6) is rewritten as $R(\Delta\mu) = \ln R(I+2, I, A) - \Delta S - \Delta\mu/T$. In Fig. 5, $R(\Delta\mu)$ is plotted for typical reactions as a function of ΔB for the isobar combinations of $I = (7, 5)$ and $I = (9, 7)$. T and $\Delta\mu$ are taken from Fig. 4. For the ^{64}Ni reaction, $R(\Delta\mu)$ values are slightly larger than those predicted by the average T. The mass range of the isotopes with $I = (7, 5)$ and (9,5) for ^{64}Ni reaction is $A = 25$ to 63. It was pointed out earlier that the analysis using $A < 50$ isobars has large uncertainty due to large Δ_{T0} when $T \geqslant 3$ MeV. Using the calculation of Δ_{T0} shown in Fig. 1, the experimental $\Delta B(0)$ of isobars are temperature corrected for $T = 2$ and 3 MeV, which are labeled as $\Delta B(T)^*$. After the temperature correction, the correlation between the isobar combinations of $I = (7, 5)$ and $I = (9, 7)$ and the temperature-corrected $\Delta B(T)^*$ are plotted in Fig. 5. It is easy to see that for the ^{48}Ca reaction, T from $\Delta B(2)^*$ and $\Delta B(3)^*$ decrease to 1.56 ± 0.12 MeV and 1.27 ± 0.10 MeV, respectively. For other reactions, T from the temperature-corrected $\Delta B(T)^*$ are only slightly modified. The correlation between the $I = (7, 5)$ and $I = (9, 7)$ IYRs and $\Delta B(3)^*$ for the ^{64}Ni reaction overlap with $\Delta B/T$. It can be concluded that T extracted from IYR of small mass is greatly affected by $\Delta B(T)^*$.

In Refs. [30,31,33,52], different temperatures ($T = 2.2$, 6.0, and 9.5 MeV) are used. Compared to other works, a relatively low $T = 2.2$ MeV was used to estimate the binding energies of very neutron-rich copper isotopes [30] in the 64A MeV ^{86}Kr + ^{9}Be reaction [43]. The staggering in the isotopic yield is minimized by introducing the approximation of back-shifted Fermi gas level density, or a parameter ε. In Fig. 2, T and $\Delta\mu$ obtained from all the IYRs is $T = 1.97 \pm 0.10$ and -3.16 ± 0.26 MeV, respectively. The dashed line represents $T = 2.2$ MeV. In Ref. [30], the equation used [Eq. (1)] to calculate the yield of a fragment (N, Z) is very similar to what we used in this article, $Y(N, Z) = CA^{3/2}\exp[(N\mu_n + Z\mu_p - F)/T]$, where F is the free energy, $\Delta\mu = -2.5$ MeV ($\mu_n = -9.5$ and $\mu_p = -7.0$ MeV), $\tau = 3/2$ is different from the MFM of $\tau = -3.6 \sim -2.2$ (minus sign) in different I values [41]. The very similar temperatures in Ref. [30] and this work indicate that temperature extracted from isobaric yield ratios is reasonable.

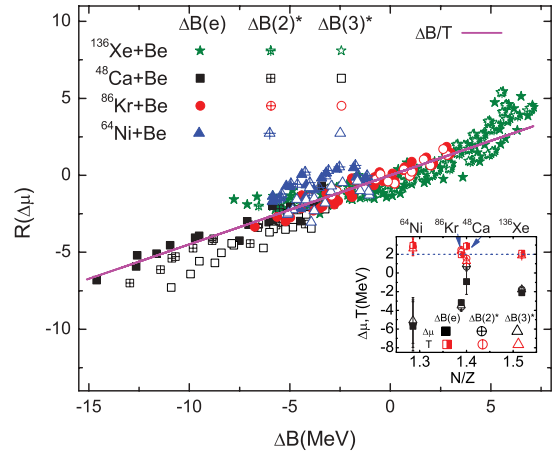

FIG. 5. (Color online) The correlation between the $R(\Delta\mu)$ and the temperature-corrected $\Delta B(T)^*$ of the $I = (7, 5)$ and $I = (9, 7)$ IYRs. The solid symbols represent the results for the experimental $\Delta B(e)$; the crossed and open symbols represent the results for the temperature-corrected $\Delta B(2)^*$ and $\Delta B(3)^*$, respectively. The lines are the fitting results using Eq. (5). The inserted figure shows the fitted values of T and $\Delta\mu$ from the original IYR [$\ln R(I+2, I, A) - \Delta S$].

Finally, we investigate the temperature of prefragment and final fragment in a modified statistical abrasion-ablation (SAA) model [53,54]. The SAA model can well reproduce the yield of fragments [49] and was used to study the isospin phenomena in HICs [55–58]. In brief, in the SAA model, the prefragment is calculated after the numbers of abraded protons and neutrons are known, which are determined by the nuclear-density distribution in the overlapping zone of projectile and target, and the nucleon-nucleon reaction cross section. Mean excitation energy of $13.3\Delta A$ MeV is assigned in the initial prefragments when ΔA numbers of protons and neutrons are removed from the projectile in the ablation-abrasion process. After the abrasion, the excited initial projectile nucleus undergoes the deexcitation process and forms the final fragment. The model description can be found in Refs. [49,53,54].

The 140A MeV ^{64}Ni + ^{9}Be and 1A GeV ^{136}Xe + ^{208}Pb reactions are calculated. The IYRs of prefragments and final fragments in the ^{64}Ni and ^{136}Xe reactions are plotted in

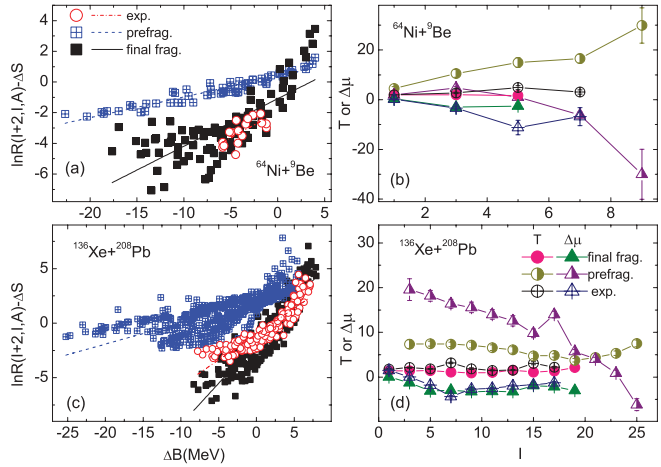

FIG. 6. (Color online) (a) IYRs for the prefragments (crossed squares) and final fragments (solid squares) in the 140A MeV ^{64}Ni + ^{9}Be reaction of the SAA result, and those for the measured fragments (open circles). (b) T (circles) and $\Delta\mu$ (triangles) determined from IYRs of the prefragments (half-full symbols), final fragments (full symbols), and the measured fragments (crossed symbols) in the 140A MeV ^{64}Ni + ^{9}Be. (c) and (d) are the same as that of (a) and (b), respectively, but for the 1A GeV ^{136}Xe + ^{208}Pb reaction.

Figs. 6(a) and 6(c), respectively. The IYRs of final fragments mostly overlap with those of the measured ones, while the IYRs of the prefragments have large differences from those of final fragments and the measured ones. T and $\Delta\mu$ determined from the IYRs with different I of prefragments and final fragments in the ^{64}Ni and ^{136}Xe reactions are plotted in Figs. 6(b) and 6(d), respectively. T from IYRs of the final fragments are very similar to those from the experimental fragments, while T from IYRs of the prefragments are rather higher than those from the experimental fragments. It is shown that the drastic modification of T and chemical potential between the prefragments and the final fragments results in the similar values in T and chemical potential extracted by the IYRs from the cold fragments in different reactions studied here. In other words, they are essentially governed by the sequential decay process. Therefore the yield of the cold fragments can be obtained by a simple scaling of Eq. (5) for a variety of reaction systems in the wide incident energy range studied in this work. The extracted T plotted in Fig. 4(a) show low T values of $1 \sim 3$ MeV. However, within that range they tend to correlate with the projectile masses, that is, T decreases as the projectile mass increases. This may reflect the difference in T of the prefragments before the secondary decays. In the SAA analysis, the excitation energy of the prefragments are given by $E^* = 13.3\Delta A$ MeV, where ΔA is the number of nucleons removed from the projectile by the ablation-abrasion process. If the prefragment is in a thermal equilibrium, T will be given by $T = \sqrt{E^*/a}$ and $a = A/k$, k is the inverse level density parameter. This leads to $T = \sqrt{13.3k\Delta A/A}$. ΔA values are similar for the reactions studied here. Therefore T becomes higher for the lighter prefragments which are produced more from the lighter projectile. However, one should note that the extracted temperatures by the IYRs from the cold fragments are significantly modified from that of the prefragments by the sequential decay process. The correlation in Fig. 4(a) merely reflects that the difference of the prefragments still sustains in some extent through the sequential decay process.

IV. SUMMARY

In summary, the temperature of a fragment after sequential decay is studied using the isobaric yield ratio method in the framework of a modified Fisher model. The difference between the binding energy of the $I \geqslant 5$ isobars at zero T $[\Delta B(0)]$ is found to be valid for substituting the value of $\Delta B(T)$ at low T. Relatively low T which range from 1 to 3 MeV are obtained in different reactions. It is shown that T depends on the neutron richness of the projectile. The mass of the target used affects T only slightly. The incident energy is found to affect T very little. $\Delta\mu$ is found to depend linearly on the N/Z of projectile, i.e., larger $\Delta\mu$ is found in reactions induced by more neutron-rich projectiles. Due to the mass of the isobars of $A < 50$, an attempt was made to use the temperature-corrected $\Delta B(T)^*$. It is found that T of the ^{48}Ca reaction, in which isobars of $A < 50$ are dominant, is largely modified by the temperature-corrected $\Delta B(T)^*$, while T of other reactions, which involve isobars of larger masses, only are slightly affected by the $\Delta B(T)^*$.

The SAA model analysis for the 140A MeV ^{64}Ni + ^{9}Be and 1A GeV ^{136}Xe + ^{208}Pb reactions revealed that the secondary decay process significantly modifies T and $\Delta\mu$ of the prefragments and governs those obtained from the cold fragments. This leads to similar IYR distributions and temperatures of cold fragments in reactions of different incident energies and different projectile masses. The SAA results also suggest that T from IYRs indeed reflect the actual physical temperature for the prefragments and the final fragments, although the latter should be viewed as a sequenced temperature of the secondary decay process in conjunction with that of the primary process. Since the MFM method should be applied to the initial hot nuclear matter in principle, the drawback of the application of this method to the final fragments is not directly to probe the characteristic nature of the initial stage, but mainly to probe that of the secondary decay processes. However, we believe that to elucidate the effect of the secondary process on the fragment yield is crucial to studying the nature of the primary emitting source, because all experimentally observed fragments have to go through this process.

ACKNOWLEDGMENTS

This work is supported by National Natural Science Foundation of China under Contracts No. 10905017 and No. 10979074, the Knowledge Innovation Project of the Chinese Academy of Sciences under Contract No. KJCX2-EW-N01, the Program for Innovative Research Team (in Science and Technology) under Contract No. 2010IRTSTHN002 in Universities of Henan Province, and the Young Teacher Project in Henan Normal University, China. One of us (R. Wada) thanks the visiting professorship of senior international scientists of the Chinese Academy of Sciences for support.

[1] A. S. Hirsch *et al.*, Phys. Rev. C **29**, 508 (1984).
[2] A.L. Goodman, J. I. Kapusta, and A. Z. Mekjian, Phys. Rev. C **30**, 851 (1984).
[3] Y. G. Ma *et al.*, Phys. Rev. C **60**, 024607 (1999).
[4] Y. G. Ma and W. Q. Shen, Nucl. Sci. Tech. **15**, 4 (2004).
[5] B. K. Srivastava *et al.* (EOS Collaboration), Phys. Rev. C **65**, 054617 (2002).
[6] C. B. Das *et al.*, Phys. Rev. C **66**, 044602 (2002).
[7] Y. G. Ma *et al.*, Phys. Rev. C **69**, 031604(R) (2004).
[8] Y. G. Ma *et al.*, Phys. Rev. C **71**, 054606 (2005).
[9] N. K. Glendenning, L. P. Csernai, and J. I. Kapusta, Phys. Rev. C **33**, 1299 (1986).
[10] M. Baldo and L. S. Ferreira, Phys. Rev. C **59**, 682 (1999).
[11] M. B. Tsang, W. A. Friedman, C. K. Gelbke, W. G. Lynch, G. Verde, and H. Xu, Phys. Rev. Lett. **86**, 5023 (2001).
[12] A. S. Botvina, O. V. Lozhkin, and W. Trautmann, Phys. Rev. C **65**, 044610 (2002).
[13] A. Ono, P. Danielewicz, W. A. Friedman, W. G. Lynch, and M. B. Tsang, Phys. Rev. C **68**, 051601(R) (2003).
[14] A. Ono, P. Danielewicz, W. A. Friedman, W. G. Lynch, and M. B. Tsang, Phys. Rev. C **70**, 041604(R) (2004).
[15] S.R. Souza, M. B. Tsang, B. V. Carlson, R. Donangelo, W. G. Lynch, and A. W. Steiner, Phys. Rev. C **80**, 044606 (2009).
[16] H. Zheng and A. Bonasera, Phys. Lett. B **696**, 178 (2011).
[17] P. Zhou, W. D. Tian, Y. G. Ma, X. Z. Cai, D. Q. Fang, and H. W. Wang, Phys. Rev. C **84**, 037605 (2011).
[18] D. J. Morrissey *et al.*, Phys. Lett. B **148**, 423 (1984).
[19] J. Pochodzalla *et al.*, Phys. Rev. Lett. **55**, 177 (1985).
[20] J. B. Natowitz *et al.*, Phys. Rev. C **65**, 034618 (2002).
[21] S. Albergo *et al.*, Nuovo Cimento A **89**, 1 (1985).
[22] J. B. Natowitz *et al.*, Phys. Rev. C **52**, R2322 (1995).
[23] J. Pochodzalla *et al.*, Phys. Rev. Lett. **75**, 1040 (1995).
[24] J. Wang *et al.*, Phys. Rev. C **72**, 024603 (2005).
[25] R. Wada *et al.*, Phys. Rev. C **55**, 227 (1997).
[26] V. Serfling *et al.*, Phys. Rev. Lett. **80**, 3928 (1998).
[27] G. D. Westfall, Phys. Lett. B **116**, 118 (1982).
[28] B. V. Jacak *et al.*, Phys. Rev. Lett. **51**, 1846 (1983).
[29] J. Su, L. Zhu, W. J. Xie, and F. S. Zhang, Phys. Rev. C **85**, 017604 (2012).
[30] M. B. Tsang *et al.*, Phys. Rev. C **76**, 041302(R) (2007).
[31] G. Chaudhuri, S. Das Gupta, W. G. Lynch, M. Mocko, and M. B. Tsang, Phys. Rev. C **76**, 067601 (2007).
[32] S. Mallik, G. Chaudhuri, and S. Das Gupta, Phys. Rev. C **83**, 044612 (2011).
[33] S. R. Souza and M. B. Tsang, Phys. Rev. C **85**, 024603 (2012).
[34] M. Huang *et al.*, Phys. Rev. C **81**, 044620 (2010).
[35] C. W. Ma *et al.*, Chin. Phys. Lett. **29**, 092101 (2012).
[36] C.W. Ma, F. Wang, Y.G. Ma, and C. Jin, Phys. Rev. C **83**, 064620 (2011).
[37] C.-W. Ma *et al.*, Eur. Phys. J. A **48**, 78 (2012).
[38] C.-W. Ma *et al.*, Chin. Phys. Lett. **29**, 062101 (2012).
[39] C. B. Das, S. Das Gupta, and A. Majumder, Phys. Rev. C **65**, 034608 (2002).
[40] R. W. Minich *et al.*, Phys. Lett. B **118**, 458 (1982).
[41] M. Huang *et al.*, Phys. Rev. C **82**, 054602 (2010).
[42] S. J. Lee and A. Z. Mekjian, Phys. Rev. C **82**, 064319 (2010).
[43] M. Mocko *et al.*, Phys. Rev. C **76**, 014609 (2007).
[44] G. Audi, A. H. Wapstra, and C. Thibault, Nucl. Phys. A **729**, 337 (2003).
[45] D. Henzlova *et al.*, Phys. Rev. C **78**, 044616 (2008).
[46] J. Reinhold *et al.*, Phys. Rev. C **58**, 247 (1998).
[47] V. Föhr *et al.*, Phys. Rev. C **84**, 054605 (2011).
[48] M. Mocko *et al.*, Phys. Rev. C **74**, 054612 (2006).
[49] C. W. Ma *et al.*, Phys. Rev. C **79**, 034606 (2009).
[50] J. Su and F. S. Zhang, Phys. Rev. C **84**, 037601 (2011).
[51] W. Trautmann *et al.* (ALADIN Collaboration), Phys. Rev. C **76**, 064606 (2007).
[52] C. B. Das *et al.*, Phys. Rep. **406**, 1 (2005).
[53] T. Brohm and K.-H. Schmidt, Nucl. Phys. A **569**, 821 (1994).
[54] D. Q. Fang *et al.*, Phys. Rev. C **61**, 044610 (2000).
[55] C.-W. Ma, H.-L. Wei, and M. Yu, Phys. Rev. C **82**, 057602 (2010).
[56] C. W. Ma *et al.*, Chin. Phys. B **18**, 4781 (2009).
[57] C. W. Ma *et al.*, J. Phys. G: Nucl. Part. Phys. **37**, 015104 (2010).
[58] C. W. Ma and S. S. Wang, Chin. Phys. C **35**, 1017 (2011).